JOURNAL OF APPLIED ELECTROCHEMISTRY 8 (1978) 195–205

Characterization of reticulate, three-dimensional electrodes

A. TENTORIO, U. CASOLO-GINELLI

Divisione Ricerca e Svilippo, Istituto Ricerche G. Donegani, Montedison Via del Lavoro, 4, 28100 Novara, Italy

Received 2 June 1977

A study has been made of the mass transfer characteristics of a reticulate, three-dimensional electrode, obtained by metallization of polyurethane foams. The assumed chemical model has been copper deposition from diluted solutions in 1 M H_2SO_4. Preliminary investigations of the performances of this electrode, assembled in a filter-press type cell, have given interesting results: with 0·01 M $CuSO_4$ solutions the current density is 85 mA cm^{-2} when the flow rate is 14 cm s^{-1}.

List of symbols

- a area for unit volume (cm^{-1})
- C copper concentration (mM cm^{-3})
- C_L copper concentration in cathode effluent (mM cm^{-3})
- C_0 copper concentration of feed (mM cm^{-3})
- C_0^0 initial copper concentration of feed (mM cm^{-3})
- d pore diameter (cm)
- D diffusion coefficient ($cm^2 s^{-1}$)
- F Faraday's constant (mcoul me_q^{-1})
- i electrolytic current density on diaphragm area basis (mA cm^{-2})
- I overall current (mA)
- K_m mass transfer coefficient (cm s^{-1})
- n number of electrons transferred in electrode reaction (me_q mM^{-1})
- P volumetric flux ($cm^3 s^{-1}$)
- Q total volume of solution (cm^3)
- (Re) Reynold's number
- S section of electrode normal to the flux (cm^2)
- (Sc) Schmidt's number
- (Sh) Sherwood's number
- t time
- T temperature
- u linear velocity of solution (cm s^{-1})
- V volume of electrode (cm^3)
- ∇ divergence operator
- ϵ void fraction
- λ $\frac{u}{K_m a \epsilon}$ (cm)
- σ electrical specific conductivity of electrolyte ($\Omega^{-1} cm^{-1}$)
- ϕ_S potential of the solution (mV)
- ρ density of the solution (g cm^{-3})
- ν kinematic viscosity ($cm^2 s^{-1}$)

1. Introduction

It is well known that one of the limiting factors to the employment of electrochemical processes is the low space–time yield of the conventional electrolysis cells and the subsequent high investment cost.

Attempts to overcome this handicap were made by the introduction of three-dimensional electrodes (fluidized bed [1] or packed bed [2]), which, by means of the increase of surface per unit volume and of mass transfer coefficient, are able to give higher specific capacities.

The drastic reduction of investment costs thus obtained gives the opportunity of putting forward an electrochemical alternative for those processes in which variable costs play a non-determining role: for example, this is the case for waste water treatment or organic fine chemical synthesis [3–5].

Packed and fluidized bed electrodes are already known and widely described [1, 2, 6, 7, 14]. Below we give a description and a characterization of a three-dimensional electrode, obtained by means of the electroless metallization of expanded, reticulate, polyurethane.

Owing to its particular geometry, this electrode

is applicable for mass-transfer controlled reactions; it has been characterized by studying copper deposition from diluted solutions in 1 M H_2SO_4, a very well-known model [2, 7–10].

2. Electrode description

The electrode is obtained by means of the electroless copper plating of expanded, reticulated polyurethane (Fig. 1).

Electroless copper plating consists in a chemical reduction of copper salts with formaldehyde on surfaces activated by treatments with $SnCl_2$ and $PdCl_2$; details of this operation are already known [11].

The thin layer of copper so obtained (about 0·3 μm) is sufficient to confer electrical conductivity to the matrix and so it is possible to reinforce the layer by means of the galvanic deposition of copper. The electrode retains practically the same geometry of the initial polyurethane and has good mechanical properties as well as lightness. The specific surface of the electrode depends on the porosity of the initial plastic matrix and on the galvanic deposition procedures.

Coulometric measurements, carried out according to Vashkyalis and Kimtene [12], give mean values from 6 cm^{-1} for polyurethane foams with 10 pores per inch (ppi) to 25 cm^{-1} for foams with 60 ppi when the current density of copper deposition was maintained roughly constant for all the foams. These values are quite low, if compared with the specific surfaces of other types of electrodes [11]. However, in practice, with the same concentration of reagent the current supplied by this electrode is comparable with that given, for example, by fluidized bed electrodes. This is possible owing to the low pressure drops of the solution throughout the electrode. To sum up, high flow rate and high mass transfer are available with low pumping energy.

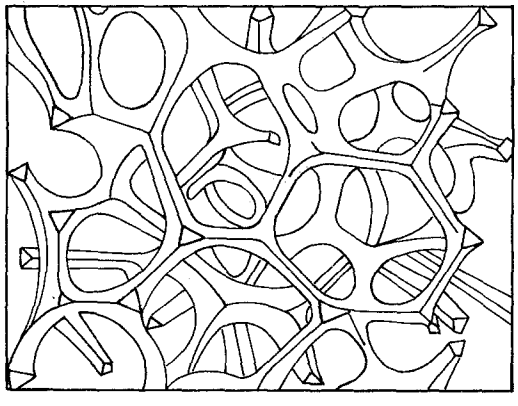

Fig. 1. Enlarged view of the electrode.

3. Theory

3.1. *General aspects*

The description of the electrode is made on the basis of the following assumptions:

(i) The reaction is mass-transfer controlled, i.e. the current depends on the transport of Cu^{2+} and not on the electrode potential;

(ii) The electrical resistivity of the electrode is negligible with respect to that of the solution.

The equations, describing the system in the general three-dimensional case, are the following:

(a) Mass-balance over a differential element of electrode, considered fictitiously 'void', with a proper correction of local fluid velocity (u/ϵ) and concentration (ϵC)

$$\nabla uC = -K_m a \epsilon C \tag{1}$$

(b) Faraday's law

$$\nabla i = -nF\nabla uC \tag{2}$$

(c) Divergence theorem

$$I = \iiint_V \nabla i \, dx \, dy \, dz \tag{3}$$

(d) Ohm's law

$$i/\epsilon = -\sigma \operatorname{grad} \phi_S . \tag{4}$$

These equations describe a stationary system in which the concentration is independent of time; they are valid for a single-pass process or when, operating with a recycle of solution, the concentration is maintained artifically constant.

In practice this latter situation has been reproduced by means of a copper anode which dissolves with unitary current efficiency.

In the case of a multiple-pass process, with diminishing copper concentration, it is necessary to take into account a mass-balance calculated for the overall volume of the solution.

Not taking into account the initial transient

(equal concentration throughout the electrode)

$$Q\frac{dC_0}{dt} = SuC_L - SuC_0. \quad (5)$$

In the following paragraphs integration of the set of differential equations will be carried out, with the boundary conditions related to two different systems: current parallel to the flux and current perpendicular to the flux of the solution.

3.2. *Current parallel to the flux of solution*

Assuming a flat profile of velocity, the matter is typically one-dimensional and similar to that dealt with by Fleischmann *et al.* [7].

Under the following boundary conditions

$$\begin{cases} x = 0 \\ C = C_0 \end{cases} \quad \text{and} \quad \begin{cases} x = 0 \\ i = 0 \end{cases}$$

concentration and current density vary with respect to the distance x according to

$$C(x) = C_0 \exp(-x/\lambda) \quad (6)$$

and

$$i(x) = nFuC_0[1 - \exp(-x/\lambda)]. \quad (7)$$

The overall current can be obtained by the integration of Equation 3 between the limits 0 and x_1, 0 and y_1, 0 and z_1 (taking into account a parallelepiped with volume $x_1 y_1 z_1$)

$$I = nFuSC_0[1 - \exp(-x_1/\lambda)]. \quad (8)$$

When the solution is continuously recycled throughout the electrode, with progressively diminishing concentration, we can assume as boundary condition

$$\begin{cases} t = 0 \\ C_0 = C_0^0. \end{cases}$$

Concentration and current vary with time as follows

$$C_0 = C_0^0 \exp\{-(Sut/Q)[1 - \exp(-x_1/\lambda]\} \quad (9)$$

and

$$I = nFuSC_0^0[1 - \exp(-x_1/\lambda)] \times \exp\{-(Sut/Q)[1 - \exp(-x_1/\lambda)]\}. \quad (10)$$

The overall current diminishes in an exponential way with time; the value of K_m can be obtained from either the intercept or the slope of the plot $\ln I$ v. t.

Potential distribution in the electrolyte can be obtained by integration of Equation 4 with boundary conditions

$$\begin{cases} x = x_1 \\ \phi_S = 0. \end{cases}$$

Limiting the integration, for the sake of simplicity, to only the stationary case (concentration independent from time)

$$\phi_S(x) = \frac{nFuC_0}{\epsilon\sigma}(x_1 - x) + \frac{nFuC_0\lambda}{\epsilon\sigma}[\exp(-x_1/\lambda) - \exp(x/\lambda)] \quad (11)$$

and the overall ohmic drop between the limits $x = 0$ and $x = x_1$

$$[\Delta\phi_S]_{x_1}^0 = \frac{nFuC_0}{\epsilon\sigma}x_1 - \frac{I\lambda}{S\epsilon\sigma}. \quad (12)$$

Owing to the high electrical conductivity of the electrode, the variations of the electrode potential are practically due only to the ohmic drop in the solution filling the electrodic volume. This ohmic drop must not be greater than the potential range in which the reaction occurs with good current efficiency and relatively high current density; that is, to a good approximation in the case of dilute solutions, the potential range in which the reaction is under diffusion control.

Providing the latter is known, Equation 12 gives a criterion to define the maximum electrodic thickness: it will be the value of x_1 which equates $[\Delta\phi_S]_{x_1}^0$ with the potential range of diffusion kinetic control.

3.3. *Current perpendicular to the flux of the solution*

In the diffusion kinetic regime, the concentration diminution inside the electrode depends only on the geometry of the electrode itself and on the hydrodynamic characteristics of the solution. Hence, assuming the vector **u** along the x-axis, $C(x)$ is still given by Equation 6. The vector **i**, laid along the y-axis, can be evaluated by integration of Equation 2 with the boundary conditions $y = 0$, $i = 0$. Owing to the fact that the only components

of **i** and **u** are i_y and u_x

$$\mathbf{i}(x, y) = \frac{nFu}{\lambda} C_0 y \exp(-x/\lambda). \quad (13)$$

Substituting in Equation 3 and integrating, one obtains again Equation 8: hence, in the diffusion kinetic regime, the overall current is independent of the relative orientation of vectors **i** and **u**.

For the same reason, the diminution of concentration and current as a function of time will still be given by Equations 9 and 10.

The variation of ϕ_S along the y-axis can be obtained from the integration of Equation 4 with the boundary conditions $y = y_1, \phi_S = 0$.

$$\phi_S = \frac{nFuC_0}{2\lambda\epsilon\sigma}(y_1^2 - y^2) \exp(-x/\lambda). \quad (14)$$

Therefore the potential in the solution (and consequently the ohmic drop) is an exponential function of x.

Limiting the evaluation of the maximum allowable thickness y_1 at the plane of maximum current density (i.e. $x = 0$)

$$[\Delta\phi_S]_{y_1}^0 = \frac{nFuC_0}{2\lambda\sigma\epsilon} y_1^2. \quad (15)$$

Equation 8 allows the definition of an optimum criterion for cell design.

We can reasonably assume that investment costs are proportional to the electrode volume ($V = x_1 y_1 z_1$) and to the dimension of the pumping system [i.e. to the volumetric flux $P = u y_1 z_1 = (V/x_1) u$].

With the same investment costs, expressing the parameters in Equation 8 as a function of x_1 where $u = (P/V)x_1$, $S = V/x_1$ and λ proportional to $x_1^{-1/2}$ (because, as will be shown later, K_m is almost proportional to $u^{1/2}$), it is easy to see that, with the same volume and volumetric flux, the higher x_1 the higher the current.

It is evident from Equations 12 and 15 that an increase of x_1 causes an increase of $\Delta\phi_S$ in the case of the parallel orientation of **i** and **u**, and a decrease of $\Delta\phi_S$ in the case of perpendicular orientation. The latter is therefore the best possible orientation; the limit to the increase of x_1 is given by the pressure drops of the solution along the electrode (u is proportional to x_1).

3.4. *Evaluation of K_m*

The mass transfer coefficient is a qualified parameter for the characterization of the electrode.

A first method of evaluation has already been defined by means of the slope or the intercept of the plot ln I v. t. Another method is based upon the measurement of stationary current when the copper concentration remains constant with time: in this situation, the current is given by Equation 8 and, provided x_1/λ is very low (therefore, small thickness of electrode and high velocity), by the series expansion of Equation 8

$$I = nFaC_0 V K_m \epsilon. \quad (16)$$

Thus, I results in a linear function of K_m.

The dependence of K_m on u can be expressed in terms of the following dimensionless parameters

$$(Sh) = K_m d/D = Id/(nFaVC_0\epsilon D)$$

$$(Sc) = \nu/D$$

$$(Re) = ud/(\epsilon\nu).$$

We have considered a relation of the type

$$(Sh) = \alpha(Sc)^{1/3}(Re)^{\beta}$$

where the exponent of (Sc) has been chosen, *a priori*, according to a totally accepted opinion, and α and β are constants which can be evaluated experimentally.

4. Experimental

4.1. *Current parallel to the flux of solution*

The electrolytic cell is shown in Fig. 2; the hydraulic circuit was completed by a tank, a pump and a flowmeter. The cell had two different anodes; the first, made of copper and inserted in the hydraulic circuit of the solution, was used in experiments carried out at constant concentration, and the second, a platinum-disc separated by means of a cationic membrane Amfion C-100, was used during the deaeration and the tests with decreasing concentrations of copper. The cathode was made of 10 or 20 ppi polyurethane foam, plated in two steps:

(i) Electroless copper plating by means of a reduction of Cu^{2+} with formaldehyde, provided

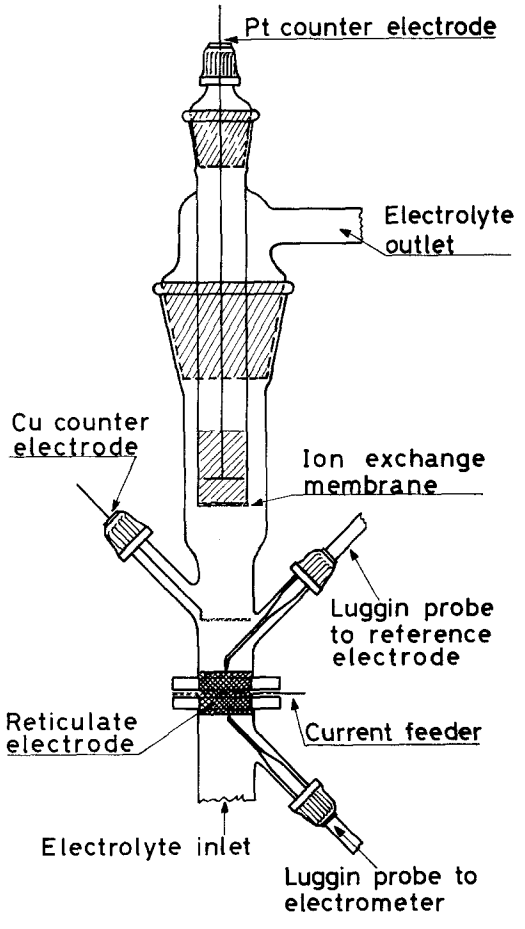

Fig. 2. Schematic view of the cell with electrodic volume of 3·5 cm^3.

the polyurethane foams are activated with solutions of $SnCl_2$ and $PdCl_2$:
(ii) Galvanic copper plating with a conventional acid solution of $CuSO_4$ and with a diaphragm current density of 450 mA cm^{-2} (10 ppi) or 550 mA cm^{-2} (20 ppi) for 20 min.

The cathode had a cylindrical shape, 2·1 cm in diameter and 1 cm in height. The reference electrode was $Hg/Hg_2SO_4/H_2SO_4$ 0·1 N; a second reference electrode, with the same chemical composition and connected to a Luggin capillary placed on the opposite side of the foam, allowed the measurement of ohmic drop $\Delta\phi_S$ and, hence, the control of the kinetic regime throughout the electrode.

The electrolyte was 1 M H_2SO_4 with 200 ppm of Cu^{2+}; the solution was continuously recycled at a constant prefixed rate.

The electrolyte was carefully deaerated by means of a continuous bubbling of nitrogen in the tank and pre-electrolysis. The latter was carried out in the same hydraulic circuit, before the addition of Cu^{2+}, using the foam as a potential-controlled cathode (− 800 mV v. $Hg/Hg_2SO_4/H_2SO_4$ 0·1 N) and the platinum disc as anode.

The deaeration was carried out until a residue current of 100 μA was reached, then a concentrated solution of $CuSO_4$ was added in order to obtain the desired copper concentration.

Instruments used were a 551/SU Amel potentiostat, a 560 Amel adapter and a Speedomax W recorder; ohmic drops were measured by means of a 667/RM Amel electrometer.

4.2. *Current perpendicular to the flux on the solution*

In this case the cell has completely different dimensions and design (an exploded view is given in Fig. 3). It is made with a PVC frame which encloses the three-dimensional electrode and in which an electrolyte inlet and outlet are provided. A cationic membrane and a PVC foil are placed on opposite sides of the electrode; a Luggin probe, inserted in the PVC foil, provides electrical connection to the reference electrode.

The flux of the solution is upward to allow a vent for gases which occasionally form at the electrode.

The anolyte is enclosed in the volume defined by the membrane, the anode and a second frame; another PVC foil adheres to the anodic surface not in contact with the anolyte. Teflon gaskets ensure an hydraulic seal and all the components are joined by means of two terminal aluminium plates, not shown in the figure, provided with suitable holes for screws and nuts.

The dimensions of the electrode are 10 × 10 × 1 cm^3 and its galvanic plating needs particular attention in order to obtain reproducible values of specific surface and throwing power.

Galvanic copper deposition was carried out in 2 steps:

(i) With a pyrophosphate bath of pH = 8–8·5; 30 mA cm^{-2} for 1 h.
(ii) With an acid bath of $CuSO_4$; 70 mA cm^{-2} for

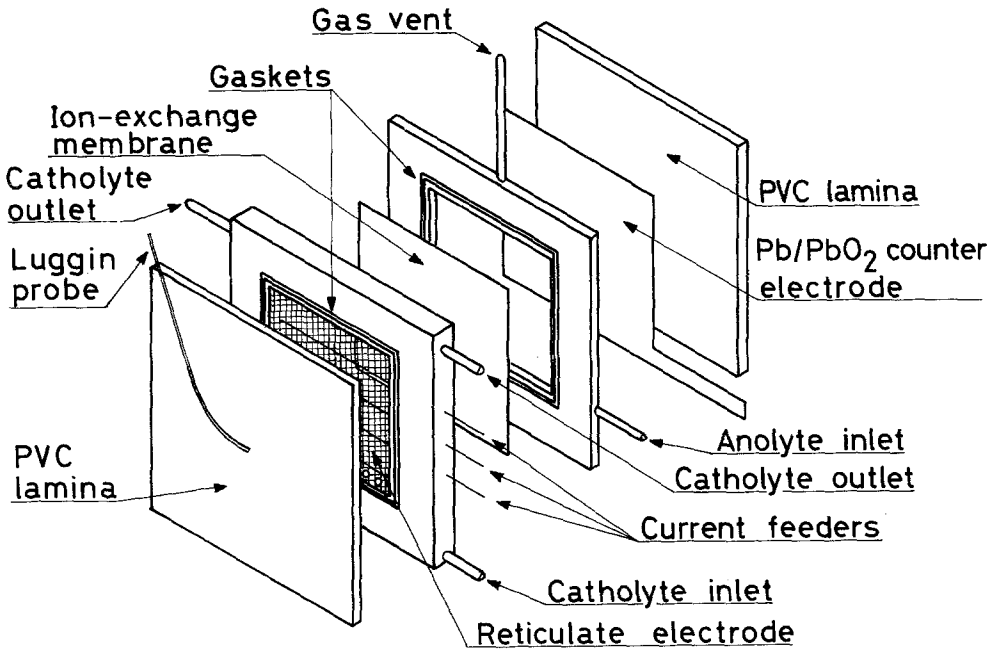

Fig. 3. Exploded view of the cell with electrodic volume 100 cm^3.

10 ppi electrodes, and 90 mA cm^{-2} for 20 ppi electrodes, for 1 h.

The counter electrode was a Pb foil, covered by PbO_2 and the reference electrode was $Hg/Hg_2SO_4/H_2SO_4$ 0·1 N.

The hydraulic circuit was completed by a tank, a flowmeter, a centrifugal pump, and a water-cooling coil.

The electrolyte (H_2SO_4 1 M) was deaerated in the aforementioned way, by continuous bubbling of nitrogen and by pre-electrolysis carried out until a residue current of about 100 $\mu A\ cm^{-2}$; then a concentrated copper sulphate solution was injected to give the final desired concentration (normally 200 ppm).

The solution was recycled throughout the electrode at a constant and prefixed rate, at a temperature of 25°C.

Electrolysis was stopped when the current was an order of magnitude higher than the pre-electrolysis current (1 mA cm^{-2}). Copper concentration was analysed at the start and at the end of the electrolysis by means of atomic adsorption spectrometry.

The anolyte was 1 M H_2SO_4, isolated from the hydraulic circuit by means of a cationic membrane The anodic compartment was kept full by the attachment of a reserve tank. The current was supplied by a 551 Amel potentiostat and was recorded by the aforementioned adapter and recorder.

A different experiment, devoted to a definition of the potentiality of the cell and to a comparison with other electrolytic cells (summarized recently by Houghton and Kuhn [15]), was made with a 0·01 M $CuSO_4$ solution in 1 M H_2SO_4, in a cell whose cathode (10 x 10 x 1 cm^3; 20 ppi copper-plated polyurethane) and anode (copper goal) were both inserted in the hydraulic circuit, in order to obtain a constant copper concentration. In this case, the deaeration of the solution was carried out only by prolonged bubbling of nitrogen; the flow rate was 14 cm s^{-1} and temperature 25° C.

The current was supplied by a d.c. generator Mediwest 24 (Westinghouse) and was monitored using a suitable shunt, a 667/RM Amel Electrometer and a Speedomax W recorder.

5. Results

5.1. *Polarization curves*

Linear sweep voltammetry (20 mV min^{-1}) was carried out to evaluate the different kinetic

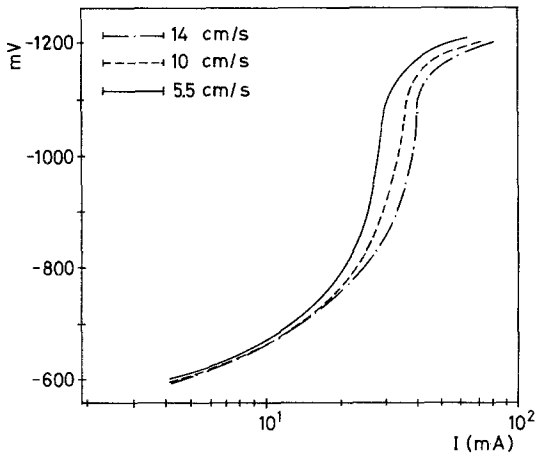

Fig. 4. Polarization curves at various flow rates for the reduction of a 200 ppm Cu^{2+} solution onto a copper goal cathode. Scanning rate, 20 mV min^{-1}.

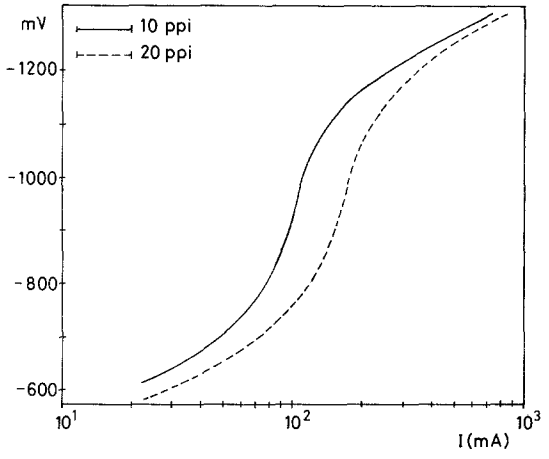

Fig. 5. Polarization curves at flow rate of 14 cm s^{-1} for the reduction of 200 ppm Cu^{2+} solution onto copper reticulate cathodes with different ppi. Scanning rate, 20 mV min^{-1}.

regimes as functions of electrode potential and of flow rate of the diluted copper solution (200 ppm). The cell, which was similar to that shown in Fig. 2, has a two-dimensional net (2·1 cm in diameter, 12 mesh) of copper as a cathode instead of a copper plated polyurethane foam. In this way the electrode potential is maintained constant throughout the electrode.

With a 200 ppm Cu^{2+} concentration and a flow rate of between 5·5 and 14 cm s^{-1}, the region of diffusion-control seems to be quite large (Fig. 4), from − 800 mV to − 1100 mV (all the potentials are with respect to $Hg/Hg_2SO_4/H_2SO_4$ 0·1 N).

However, starting at − 950 mV a notable H^+ reduction occurs. In fact, in prolonged potentiostatic tests (950 mV), with a copper anode, the current increased regularly with a progressive darkening of the electrode and with a greater and greater H_2 evolution. At the end of the test, the electrode was completely brown, with a powdered and incoherent deposit. Probably the phenomenon is due to the fact that, in the diffusion regime, copper deposition is dendritic in nature, and increases the surface available for H^+ reduction, while copper ions, in low concentration, find access to the inside of an irregular deposit difficult.

Furthermore, H^+ reduction may lead to a local alkalinity of the solution, with a possible precipitation of cuprous oxide/hydroxide, which contributes towards making the deposit incoherent. As a matter of fact, copper reduction, at low concentration, occurs under a diffusion-controlled regime and with a faradaic efficiency near unity at potentials between − 800 and − 900 mV. This range of potential is sufficiently high to insure that the copper deposition process is also under mass-transfer control for three-dimensional electrodes (2·1 cm in diameter, 1 cm in height).

Fig. 5 shows the current–potential behaviour for copper deposition from 200 ppm Cu^{2+} at a flow rate of 14 cm s^{-1}, for 10 and 20 ppi electrodes. Well-defined limiting currents are evident.

A confirmation of this has been given by the measurement of the ohmic drop throughout the electrode. With an imposed potential of − 900 mV, the ohmic drop was about 70 mV (this value also contains the uncompensated ohmic drop between the Luggin capillary and the plane x_1).

5.2. *Current parallel to the flux of the solution*

A first set of tests was carried out with constant Cu^{2+} concentration (200 ppm) in order to derive a correlation between (*Sh*) and (*Re*) which can be extrapolated.

The attainment of a stationary current required less than 1 min and so surface modifications were practically negligible during each test. The electrodes were substituted after every 8 tests. Their specific surfaces, measured at the beginning and at the end of the group of tests, were nearly constant. Reproducible mean values of 6·9 and 9·0 cm^{-1}, respectively, for 10 and 20 ppi electrodes, were determined on a group of 24 specimens.

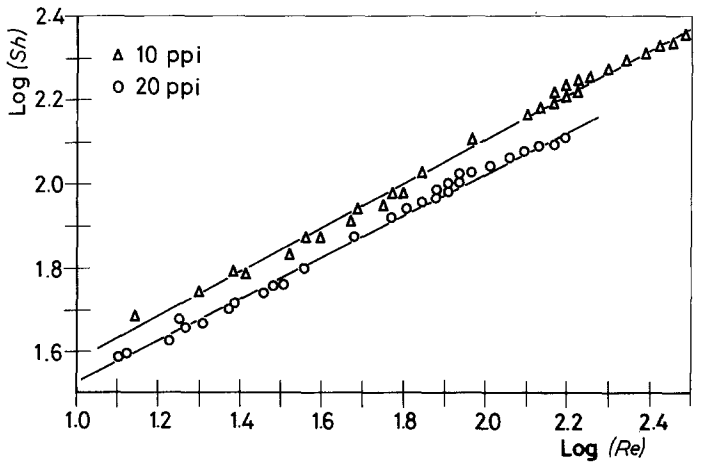

Fig. 6. (Sh)–(Re) correlations for reticulate electrodes.

Table 1. Set of values utilized in the definition of the (Sh)–(Re) correlation

d = 0·25 cm (10 ppi) / 0·12 cm (20 ppi)	e = 0·975 (10 ppi) / 0·968 (20 ppi)	a = 6·9 cm^{-1} (10 ppi) / 9·0 cm^{-1} (20 ppi)
$c = 3{\cdot}15 \times 10^{-3}$ mM cm^{-3}	$\nu = 0{\cdot}995 \times 10^{-2}$ $cm^2 s^{-1}$	$n = 2$ $me_q mM^{-1}$
$F = 96500$ mC me_q^{-1}	$D = 6{\cdot}3 \times 10^{-6}$ $cm^2 s^{-1}$	$V = 3{\cdot}5$ cm^3

Since the (Sh) value has been obtained from the stationary current at an electrode potential of − 900 mV, the validity of the (Sh)–(Re) correlation is limited by the validity of Equation 16.

x_1 being low (1 cm), even assuming unrealistically high K_m values (10^{-2} cm s^{-1}), the error arising from stopping the series expansion of Equation 8 at the first term is about 3% at the lowest tested flow rate (1 cm s^{-1}). (Sh) values as a function of (Re) are plotted in Fig. 6, for 10 and 20 ppi electrodes.

The set of values utilized in the correlation is given in Table 1. The ν value was obtained from International Critical Tables while the D value was calculated from the equation proposed by Arvia *et al.* [16]

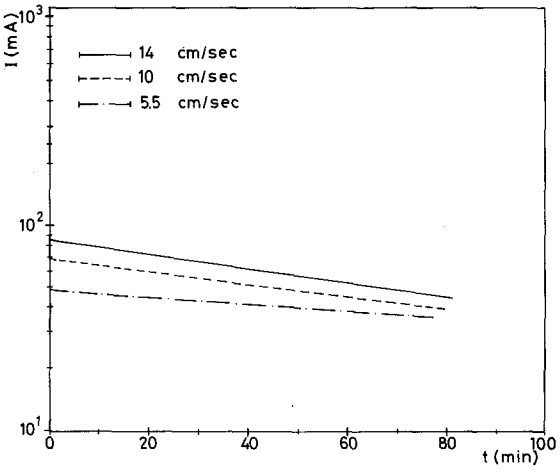

Fig. 7. Current–time behaviour at various flow rates for 10 ppi, 3·5 cm^3 electrodes.

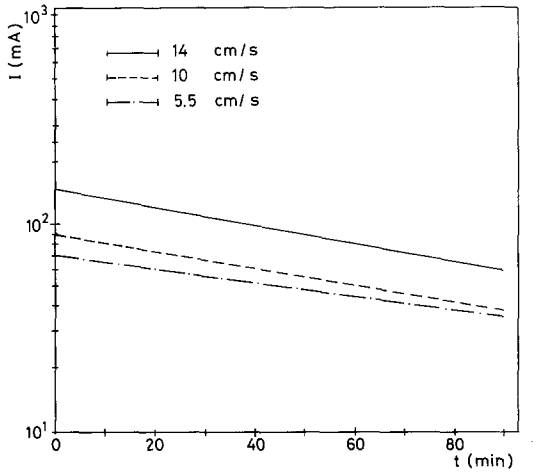

Fig. 8. Current–time behaviour at various flow rates for 20 ppi, 3·5 cm^3 electrodes.

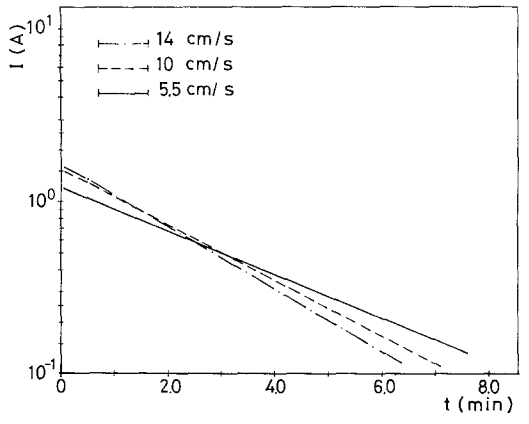

Fig. 9. Current–time behaviour at various flow rates for 10 ppi, 100 cm³ electrodes.

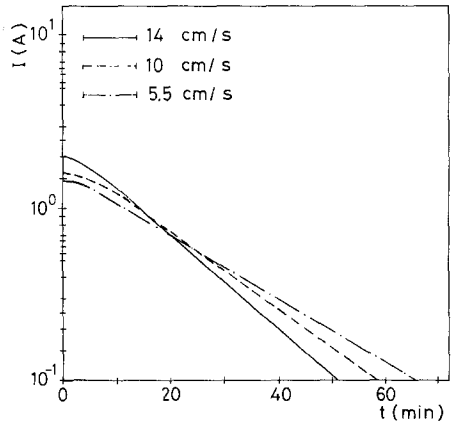

Fig. 10. Current–time behaviour at various flow rates for 20 ppi, 100 cm³ electrodes.

$$\frac{Dv}{\rho T} = (2{\cdot}23 \pm 0{\cdot}37) \times 10^{-10}\,\mathrm{cm^2\,poise\,K^{-1}}.$$

The (Sh)–(Re) correlations, obtained by a non-linear regression programme, are

$$(Sh) = 0{\cdot}99(Sc)^{0.33}(Re)^{0.53} \qquad (18)$$

with a mean error of 3·71% for 10 ppi electrodes and

$$(Sh) = 0{\cdot}95(Sh)^{0.33}(Re)^{0.49} \qquad (19)$$

with a mean error of 3·98% for 20 ppi electrodes.

Because of the limitation of the experiments to only two types of foam, it is not possible to generalize the correlation (Sh)–(Re), introducing, for example, a shape factor which describes the complex geometry of the electrode better (pores have variable dimensions and orientations; d is necessarily a mean value). On the other hand, plugging phenomena can drastically limit the significance of tests carried out with electrodes having a greater number of pores per inch. However, in both cases,

Table 2. Comparison between K_m derived from the slope of ln I v. t (K_m experimental and K_m calculated from the (Sh)–(Re) correlation in the case of small volume electrode, 3·5 cm³)

(ppi)	u (cm s^{-1})	K_m exptl. (cm s^{-1})	K_m calc. (cm s^{-1})
10	5·5	$3{\cdot}6 \times 10^{-3}$	$4{\cdot}0 \times 10^{-3}$
10	10·0	$5{\cdot}8 \times 10^{-3}$	$5{\cdot}5 \times 10^{-3}$
10	14·0	$6{\cdot}6 \times 10^{-3}$	$6{\cdot}6 \times 10^{-3}$
20	5·5	$5{\cdot}0 \times 10^{-3}$	$4{\cdot}6 \times 10^{-3}$
20	10·0	$6{\cdot}2 \times 10^{-3}$	$6{\cdot}1 \times 10^{-3}$
20	14·0	$6{\cdot}9 \times 10^{-3}$	$7{\cdot}2 \times 10^{-3}$

the exponent of (Re) agrees reasonably with that of Levich's theory [17].

A first confirmation of the validity of Equations 18 and 19 is given by the results of tests carried out with a progressive decrease of Cu^{2+} concentration (C_0^0 about 200 ppm), in the cell of Fig. 2 with a platinum anode and with an electrode potential equal to − 900 mV.

Figs. 7 and 8 (for 10 and 20 ppi electrodes respectively) show an exponential decrease of the current as a function of time, while Table 2 gives a comparison between the experimental K_m value, obtained from the sloped ln I versus t and K_m calculated from Equations 18 and 19. The agreement is satisfactory, especially at high flow rate.

5.3. *Current perpendicular to the flux of solution*

Figs. 9 and 10 show, for 10 and 20 ppi electrodes, respectively, the current–time behaviour for electrolysis carried out in the cell of Fig. 3, with an initial Cu^{2+} concentration equal to about 200 ppm and an electrode potential of − 850 mV.

Since the Luggin capillary is placed on the plane $y = 0$, this value of electrode potential should allow no H^+ reduction on the plane $y = y_1$, where the potential is more cathodic. As a matter of fact, current efficiency, determined from the quantity of current passed and the difference between the initial and final Cu^{2+} concentrations was always nearly 100%. The values of specific surface area are lower than those measured for electrodes of smaller volume; this is probably due to the different procedures of galvanic deposition.

For electrodes with 10 ppi, the values of specific

Table 3. Comparison between K_m derived from the slope of lnI v. t (K_m exptl) and K_m calculated from the (Sh)–(Re) correlation, in the case of electrodes with volume equal to 100 cm³

(ppi)	u (cm s^{-1})	K_m exptl. (cm s^{-1})	K_m calc. (cm s^{-1})
10	5·5	$4{\cdot}4 \times 10^{-3}$	$4{\cdot}0 \times 10^{-3}$
10	10·0	$5{\cdot}6 \times 10^{-3}$	$5{\cdot}5 \times 10^{-3}$
10	14·0	$6{\cdot}5 \times 10^{-3}$	$6{\cdot}6 \times 10^{-3}$
20	5·5	$4{\cdot}8 \times 10^{-3}$	$4{\cdot}6 \times 10^{-3}$
20	10·0	$6{\cdot}5 \times 10^{-3}$	$6{\cdot}1 \times 10^{-3}$
20	14·0	$7{\cdot}1 \times 10^{-3}$	$7{\cdot}2 \times 10^{-3}$

surface turned out to be quite reproducible (5·7–5·9 cm^{-1}), while 20 ppi electrodes have shown rather dispersed values (from 7·0–8·4 cm^{-1}).

In Table 3, the values of K_m, obtained from the slope of ln$I$ v. t, are compared with those calculated from Equations 18 and 19.

In conclusion, these equations describe satisfactorily the behaviour of the electrodes even when not only a different orientation of **i** and **u** is realized, but also when there is a considerable expansion of electrodic volumes (3·5 cm^3 v. 100 cm^3).

6. Discussion

The cell of Fig. 3 represents, at least at a level of design criteria, a realistic model of an industrial cell. It allows a significant check of the opportunities offered by reticulate electrodes and performs as an elementary modulus from which it is possible to derive indications for eventual scale-up. Indeed, the potentiality of this cell appears interesting: for an electrolysis accomplished under the conditions chosen by Houghton and Kuhn [15] to compare various types of cells ($CuSO_4$ 0·01 M), and with a flow rate equal to 14 cm s^{-1}, the current provided by the modulus of Fig. 3

Table 4. Comparison of performances of various types of cells (according to [15])

Cell description	*Mass transport enhancement*	i_{lim} *(approx)* (mA cm^{-2})
Widely spaced parallel plates	NC*	1·3
Capillary gap (spacing 0·02–2 cm)	FC†	2·6 (25 cm s^{-1}) 8·0 (250 cm s^{-1})
Parallel plates, packed with inert beads	FC†/GF§	0·5–0·9
Parallel mesh (expanded metal)	FC†/GF§	1·0
Rotating disc	MPC‡	2·8 (120 ppm) 8·8 (1200 ppm)
Packed bed	FC†	6 (an electrode total area basis) 115 (on diaphragm basis) 57 (on cathode volume basis)
Fluidized bed	FC†	6 (on electrode area basis) 115 (on diaphragm basis) 57 (on cathode volume basis)
Reticulate electrode	FC†	10–12 (on electrode total area basis) 80–85 (on diaphragm basis) 80–85 (on cathode volume basis)

* natural convection
† forced convection
‡ mechanically promoted convection
§ gravitational flow

was 85 mA cm^{-2}, a value similar to that obtained with fluidized bed electrodes (Table 4).

Pressure drops are another important parameter of evaluation. Attempts at measurement, still outstanding, are complicated by low values (of the order of 1 mm H_2O cm^{-1} of electrode with a flow rate equal to 10 cm s^{-1}) and the arrangement of the results appears quite meaningless; however the pressure drops represent a low fraction of the power required for electrolysis.

What are the opportunities offered by this cell?

High space–time yields, in the case of three-dimensional electrodes, can be obtained with high specific surfaces (this is the case of packed bed electrodes and of the so-called 'Swiss roll' cell [13]) or with high values of mass-transfer coefficients (as in this case and in capillary gap cells). The difference between these two situations is, above all, a difference of 'extraction efficiency' defined, as in [7], by

$$(C_0 - C_L)/C_0 = 1 - \exp(-K_m a e x_1/u).$$

It is evident that high values of extraction efficiency are obtained by means of high specific surfaces and low flow rates.

These conditions are not fulfilled by the reticulate electrode, but in spite of a relatively low specific surface, it supplies high current densities owing to high flow rates together with low pressure drops. Hence, the cell of Fig. 3 could operate in waste water treatment only with multiple-pass electrolysis and the level of concentration of pollutant after treatment should not be below tens of ppm in order not to weigh down excessively the recycle.

Hence, this cell could be used for pre-treatments to a more refined purification, for example with ion-exchange resins. Prospects in the field of electrosynthesis, particularly for organic fine-chemicals, are much more promising. Attempts made in this direction, for example the reduction of *m*-nitrosulphonic acid at a concentration of 900 mg l^{-1} to *m*-aminosulphonic acid, have shown that the reticulate electrode can give currents of the order of magnitude of 1000 A m^{-2} with current efficiencies of 75–80%.

References

[1] J. R. Backhurst, J. M. Coulson, F. Goodridge, R. E. Plimley and M. Fleischmann, *J. Electrochem. Soc.* **116** (1969) 1600.
[2] D. N. Bennion and J. Newman, *ibid.* **2** (1972) 113.
[3] J. L. Fitzjohn, *Chem. Eng. Progr.* **71–2** (1975) 85.
[4] M. Fleischmann and D. Pletcher, *Chem. in Britain* **11–2** (1975) 50.
[5] J. C. Davis, *Chem. Eng.* **82–14** (1975) 44.
[6] M. Fleischmann and J. W. Oldfield, *J. Electroanalyt. Chem.* **29** (1971) 211.
[7] A. K. Chu, M. Fleischmann and G. J. Hills, *J. Appl. Electrochem.* **4** (1974) 323.
[8] S. Germain and F. Goodridge, *Electrochim. Acta* **21** (1976) 545.
[9] N. Ibl, 'Advances in Electrochem. and Electrochem. Eng.' Vol. 2, (Eds. P. Delahay and C. W. Tobias) Interscience Publ. (1962) p. 49.
[10] M. Fleischmann, J. W. Oldfield and L. Tennakoon, *J. Appl. Electrochem.* **1** (1971) 103.
[11] US Patent No. 2938805.
[12] A. Vashkyalis and D. Kimtene, *Sov. Electrochem.* (1974) 798.
[13] P. M. Robertson, F. Schwager and N. Ibl, *J. Electroanalyt. Chem.* **65** (1975) 883.
[14] J. S. Newman and C. W. Tobias, *J. Electrochem. Soc.* **109** (1962) 1183.
[15] R. W. Houghton and A. T. Kuhn, *J. Appl. Electrochem.* **4** (1974) 173.
[16] A. J. Arvia, J. C. Bazan and J. S. W. Carrozza, *Electrochim. Acta* **11** (1966) 881.
[17] V. G. Levich, 'Physicochemical Hydrodynamics' Prentice-Hall (1962).